

Optical Engineering

OpticalEngineering.SPIEDigitalLibrary.org

Effect of gamma radiation on the stability of UV replicated composite mirrors

Rafael J. Zaldivar
Hyun I. Kim
Geena L. Ferrelli

Effect of gamma radiation on the stability of UV replicated composite mirrors

Rafael J. Zaldivar, Hyun I. Kim,* and Geena L. Ferrelli
The Aerospace Corporation, El Segundo, California, United States

Abstract. Composite replicated mirrors are gaining increasing attention for space-based applications due to their lower density, tailorable mechanical properties, and rapid manufacturing times over state-of-the-art glass mirrors. Ultraviolet (UV)-cured mirrors provide a route by which high-quality mirrors can be manufactured at relatively low processing temperatures that minimize residual stresses. The successful utilization of these mirrors requires nanometer scale dimensional stability after both thermal cycling and hygrothermal exposure. We investigate the effect of gamma irradiation as a process to improve the stability of UV replicated mirrors. Gamma radiation exposure was shown to increase the cure state of these mirrors as evidenced by an increase in modulus, glass transition temperature, and the thermal degradation behavior with dosage. Gas chromatography–mass spectroscopy also showed evidence of consumption of the primary monomers and initiation of the photosensitive agent with gamma exposure. The gamma-exposed mirrors exhibited significant improvement in stability even after multiple thermal cycling in comparison with nonirradiated composite mirrors. Though improvements in the cure state contribute to the overall stability, the radiation dosage was also shown to reduce the film stress of the mirror by over 80% as evidenced using Stoney replicated specimens. This reduction in residual stress is encouraging considering the utilization of these structures for space applications. This paper shows that replicated composite mirrors are a viable alternative to conventional optical structures. © The Authors. Published by SPIE under a Creative Commons Attribution 3.0 Unported License. Distribution or reproduction of this work in whole or in part requires full attribution of the original publication, including its DOI. [DOI: [10.1117/1.OE.57.4.047102](https://doi.org/10.1117/1.OE.57.4.047102)]

Keywords: replicated; composite; mirror; radiation; stability; epoxy.

Paper 171739 received Oct. 31, 2017; accepted for publication Mar. 16, 2018; published online Apr. 10, 2018.

1 Introduction

High-quality, lightweight composite replicated mirrors have a number of potential advantages over standard glass mirrors for use in space applications. They have a lower density, tailorable mechanical properties, higher thermal conductivity, improved damage tolerance, and reduced manufacturing times over state-of-the-art glass mirrors.^{1,2} In contrast, conventional mirrors require additional postprocessing to achieve high-precision grade specifications, such as grinding, conventional polishing, single-point diamond machining, magnetic rheological finishing, and ion milling, that further increase not only the processing time and cost but also increase the possibility of fracture during the manufacturing process.³

Replicated composite mirrors are typically fabricated by utilizing a replication process by which an uncured resin is sandwiched between a composite substrate and the high-quality glass mandrel. The resin is cured in this sandwich configuration copying the perfect surface of the mandrel while the opposing interface bonds strongly to the composite substrate. Once separation has been achieved, the replicated layer (RL) can be coated with a reflective layer and a dielectric coating, and utilized for its intended application. One of the primary properties in determining the quality of a mirror is related to the surface flatness. Surface flatness is a surface accuracy specification that measures the deviation from a flat

surface. The deviations in flatness, i.e., surface figure errors (SFEs), are measured in values of waves (λ), which are multiples of the wavelength of the testing source. In this paper, RMS SFE values are reported. One fringe corresponds to $\frac{1}{2}$ of a wave. 1λ flatness is considered as typical grade, $\lambda/4$ is considered as precision grade, and $\lambda/20$ is considered as high-precision grade. Achieving high fidelity replications ($SFE = \lambda/20$) is critically dependent on the type of replicating resin used, the quality of the master, the process of application, and the type of release monolayer film applied to the mandrel material.⁴

However, even though replicated mirrors have been processed for over 30 years, literature data with respect to the dimensional stability of high-precision grade replicated composite mirrors are less well-defined than that of their heavier glass counterparts. Unlike Zerodur®, beryllium, and ULE®, composite replicated resin materials, such as epoxies, are significantly more sensitive to dimensional fluctuations caused by thermal and environmental conditions.⁵ These environmental changes may result in nanometer scale dimensional changes that affect the mirror's SFE.⁵ Recently, the effects of cure state controlled by thermal processing conditioning on the stability of these mirrors have been investigated.⁶ Increasing the cure state of the RL reduces the moisture absorption characteristics as well as increases the thermal stability of the material. However, in bonded structures, performing higher temperature processing to achieve full cure has been shown to also increase interfacial residual stresses, which ultimately

*Address all correspondence to: Hyun I. Kim, E-mail: hyun.i.kim@aero.org

negatively affects the flatness of these mirrors.⁷ Therefore, processes that improve stability while minimizing residual stresses are critical for the development of this new class of material.

One method for minimizing the residual stresses of a replicated mirror is using an ultraviolet (UV)-cured RL rather than a thermally cured system. UV room temperature (RT)-activated cationic formulations are composed primarily of cycloaliphatic epoxies that can achieve a fairly high degree of cure with minimal thermal exposure. These formulations allow dark cure, which is a continuation of cure even after UV exposure is terminated. The UV-activated cationic photoinitiator diffuses through the material and promotes further polymerization reaction of the resin.⁸ These systems also tend to have lower cure shrinkage than thermally cured systems, further minimizing cure stresses. However, the shallow penetration of visible-UV radiation limits their cure efficiency through the depth of the film. Higher energy ionizing radiation, such as gamma, x-ray, and electron beam radiation, has been shown to also affect the cure of UV-cured epoxy resins that utilize a cationic photoinitiator.^{9,10} Gamma irradiation from a ⁶⁰Co source may be used for curing and is not restricted by the depth limitations of lower energy UV sources. However, when utilizing high-energy radiation, a careful balance must exist between the two possible simultaneous reactions that may occur, resulting in chain scission and/or cross-linking during irradiation of the polymer network.^{11,12} In the last few decades, there have been successful attempts at utilizing both gamma and e-beam radiation for the cure of epoxies and acrylate-epoxy systems for use in composite manufacture.^{13,14} However, the phenomena involved in radiation degradation of polymers are quite complex and many times lead to varying final results. Spadaro et al.¹⁵ demonstrated that cycloaliphatic epoxy resins that had been cured with acid anhydrides cross-linked after irradiation and showed an increase in glass transition (T_g) from 112°C to 117°C. However, the literature describes numerous other examples of difunctional epoxies exhibiting degradation as evidenced by decreased T_g temperatures and reduced mechanical performance.¹¹⁻¹⁵

In this investigation, we have utilized a replicated radiation-cured epoxy composite to manufacture high-quality mirrors. The replicated layer (RL) was exposed to varying degrees of radiation using a ⁶⁰Co radiation ranging from 0 to 50 Mrad. The cure state, modulus, T_g temperature, and thermal degradation behavior of the exposed UV-cured material were characterized as a function of irradiation. Gas chromatography-mass spectroscopy (GC-MS) was also utilized to evaluate changes in the starting material as a function of irradiation. Stoney bimaterial specimens using the UV-cured RL were manufactured and tested as a function of radiation exposure to evaluate what contribution this process has on the residual stress of these structures. Changes in the residual stress and cure state were correlated to the stability of the mirrors. Composite mirrors were then fabricated and evaluated for stability after thermal cycling as a function of radiation exposure using Zygo analysis. The mirrors were subjected to multiple thermal cycling profiles to evaluate their hysteresis as well as the magnitude of dimensional variations observed after postradiation exposure.

2 Experimental

2.1 Replicated Mirror Fabrication

The fabrication of coupon-level replica mirrors is achieved by sandwiching a droplet of epoxy resin (~30 to 50 mg) between a substrate and a glass mandrel (50-mm diameter and 15.9-mm thick) coated with a monolayer mold release coating. The microroughness of the mandrel surface was 0.4 nm. The sandwich is held together until the cure is complete. The cured resin layer can be separated from the mandrel via the use of a monolayer release layer, whose synthesis and deposition details are elsewhere.⁴ A uniform bond line was controlled with a shim (75- μ m thick) producing a replication ~32 mm in diameter. The replicating resin layer (RL) cure was done by UV exposure through the glass mandrel and then separated at the monolayer-coated glass and RL interface. Quasi-isotropic laminates of K13C2U/RS3C cyanate ester composite laminates were used as substrates. The composite laminate was 4 mm in thickness and was cured to 177°C prior to replication. The surface roughness of the laminate was 0.19 μ m.

2.2 Epoxy Cure

The RL was cured with exposure to a 365-nm Dymax BlueWave QX4 UV source. The UV flux was 100 mW/cm². A pen source with an 8-mm head was used for constant UV illumination. Samples were exposed with the same intensity and time to achieve equal amount of UV exposure. Two cure states were used for this study. The standard cure received UV exposure through the glass mandrel for 7 min followed by immediate separation from the mandrel. The elevated cure was exposed to the UV source for 7 min, followed by 24 h of dark cure and 24 h at 45°C, and then separated from the mandrel. The amine-cured resin described in this paper was synthesized using a bifunctional bisphenol-A epoxy and cured with a polyamine hardener. The resin was cured for 2 h at 45°C.

2.3 Surface Figure Error Determination by Interferometry

The morphology of the replication surfaces was measured with a Zygo Verifire AT Laser Interferometer. Surface quality is referred to as SFE, which is an optical term corresponding to the RMS value deviation from the ideal surface. The value is presented in terms of λ , which is equivalent to 633 nm.

2.4 Glass Transition Temperature

Neat resin samples for T_g testing were cured through a glass mandrel (to simulate a replication) with a thickness ~0.5 mm. The samples were cut into rectangles (15 mm \times 5 mm) and smoothed with 240 grit sandpaper. The samples were tested with a TA Instruments Q800 dynamic mechanical analyzer (DMA) in single cantilever mode from 25°C to 200°C with a 5°C/min heating rate, 20- μ m deflection, and 1-Hz frequency. The T_g temperature was determined from the maximum of the loss modulus peak.

2.5 Thermal Gravimetric Analysis

The thermal mass loss behavior of the RL was evaluated as a function of temperature in an inert environment for both the control and the irradiated specimens. The specimens were heated at 10°C/min in a TA Instruments Discovery Unit. Five milligrams of samples were used for evaluation when scanned from RT to 600°C.

2.6 Thermal Mechanical Analysis

A TA Instruments thermal mechanical analyzer (TMA) Q400 was used to evaluate the coefficient of thermal expansion (CTE) of neat resin samples, pre- and postradiation exposure. 5.0-mil thick (12 × 12 mm) specimens were cast and placed on edge using a specially designed holder for film testing. A solid glass probe was placed on the top edge of the specimen with 0.01-N force, and the test was scanned from -50°C to 50°C in an ambient atmosphere. The ramps rate was kept constant at 10°C/min. A linear regression fit was performed to determine the CTE.

2.7 Gas Chromatography–Mass Spectroscopy

An Agilent 7890B and an Agilent 7200A quadrupole time of flight MS were used for the GC–MS analysis. The GC column was Phenomenex, Zebron ZB-1 HT, 60-m long, 0.25 mm i.d., and 0.25- μ m film thickness, and a helium carrier gas rate of 1.2 ml/min. The MS detector was set for electron impact ionization and programmed to scan the mass range from 15 to 400 m/z. The resulting mass spectral data for the compounds identified were cross referenced to the NIST14 and Wiley 10th edition MS libraries.

2.8 Gamma Radiation

J.L. Shepard high dose rate irradiator was used to expose polymer samples to gamma radiation. The chamber consists of three ⁶⁰Co rods to achieve up to 50 rads/s. A fully enclosed, positive pressure, GN2 filled box was used to keep samples in an inert environment during exposure to eliminate oxidative degradation. The area of simultaneous exposure, i.e., the size of the enclosure, was ~1 ft × 1 ft. Prior to the sample exposure, dosimetry was used to map a grid of varying dose rates at different locations. Each sample was treated to a different exposure time to match the total final dosage within 5%.

2.9 Stoney Residual Stress Experiments

To measure the residual stress, the radius of curvature on silicon wafers is initially characterized using a Zygo Verifire Laser Interferometer with a 633-nm wavelength and 0.06-nm repeatability. The wafer thickness is also measured before depositing the resin. The UV resin is mixed according to standard protocols with the addition of 1 wt. % silica particles (5 mil) for bond line control. The silicon wafers are coated on one side with the resin mixture, sandwiched between optical flats coated with a release film, and cured according to the standard protocol. Following the resin cure, the resin thickness is measured and the radius of curvature is measured with a Taylor-Hobson Form Talysurf PGI 1220 Surface Profilometer. Two-line traces orthogonal to each other were measured and averaged. All samples are purged in nitrogen for 4 days prior to radius measurements

and testing occurs in a dry environment. The radius of curvature is measured after every 10 Mrad of gamma radiation and converted to a residual stress using the Stoney thick film equation, where the subscripts “s” and “f” denote substrate and film, respectively, M is the biaxial modulus, t is the thickness, R is the radius of curvature, and \bar{y} is the neutral axis of the sample

$$\sigma = \left[\frac{M_s}{3Rt_f} \right] \left[\frac{t_s^3 - 3t_s^2 + 3t_s^2}{t_s + 0.5t_f - \bar{y}} \right].$$

3 Results and Discussion

The space environment has been shown to have a significant impact on the various materials used for satellite applications. Co⁶⁰ gamma irradiation testing can provide some insight on the sensitivity of space radiation on material properties. In the case of polymeric materials, prolonged exposure can result in significant changes due to either chain scission or additional cross-linking or a combination of both. The degree of these changes is based on a number of factors, such as the dosage experienced, the atmosphere during irradiation, and the chemistry of the material being irradiated.¹⁶ These exposures may result in changes to the mechanical, optical, and thermal behavior of the material.¹⁷ However, for the case of resin-based mirrors, nanometer scale variations in dimension after irradiation may also result in significant changes to surface wave front error (SFE) and surface roughness, which ultimately may affect final utilization.

To better understand the effect of radiation on stability, both nonirradiated and 50-Mrad exposed UV composite replicated mirrors were thermally cycled. The thermal cycle limits were chosen so that the uppermost temperature was below the Tg of the resin while the lower temperature limit subjected a degree of stress on each mirror as a function of thermal cycles. The first cycle ranged from -25°C to 50°C for 1000 cycles. The second cycle was performed after the first and ranged from -50°C to 50°C for additional 1000 cycles. The mirror was processed using our standard cure (RT), which resulted in a Tg of the replicated resin layer (RL) of ~62°C, above the uppermost temperature for both sets of cycles.

Figures 1(a)–1(d) show the Zygo analysis surface profiles for the standard (RT) UV cure mirror with no irradiation prior to thermal cycling. Each measurement was performed at the completion of each 1000 cycle step. The red areas define the segments that are higher in elevation, and the green areas are segments that are lower in the plane. As shown, the changes in SFE profile are minimal until after the second set of thermal cycles. After this exposure, the SFE shows a significant deviation from the initial flatness as evidenced in Fig. 1(d). Some of the strong indications shown are in line with the fiber orientation of the outer ply adjacent to the replicated layer. These indications were not observed until the mirror was exposed to the lowest -50°C thermal range lower limit.

The same thermal cycling protocol was then applied to an identical composite mirror that was exposed to 50 Mrad of irradiation prior to testing. Figure 2 shows the evolution of the Zygo surface profile observed after both sets of thermal cycling. As shown for this case, the overall changes are negligible with respect to SFE, even after the second set of

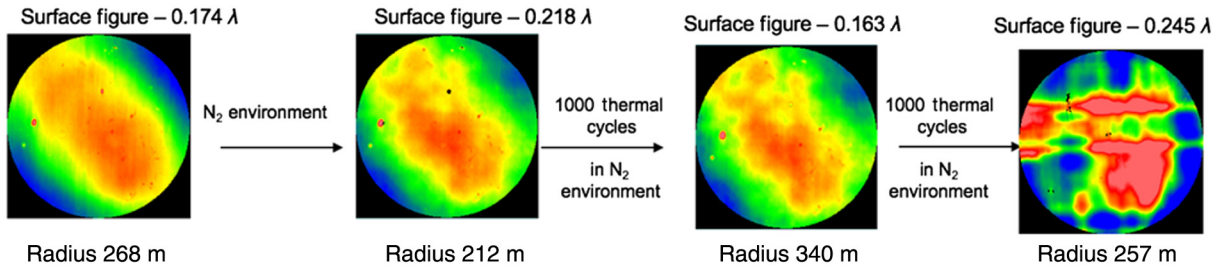


Fig. 1 Zygo analysis of standard cure (RT) UV replicated composite mirror as a function of thermal cycling. Significant deviation in SFE observed after second set (-50°C to +50°C) of thermal cycles.

1000 thermal cycles from 50°C to -50°C. This behavior in the SFE is notably different than what was observed for the nonirradiated mirrors as shown in Fig. 1. This increase in stability is clearly evident when comparing the scans shown in Fig. 1 to Fig. 2. The flatness has actually improved by 0.017λ over the initial starting condition.

To better understand the pronounced difference in mirror stability observed after the -50°C to 50°C thermal cycles for the irradiated mirrors, material properties were collected as a function of radiation exposure. Determining whether a polymer material is primarily fragmenting or further cross-linking provides valuable information with respect to the interaction of radiation with the RL. DMA was used to obtain the Tg of the replicated layer, which provides a direct correlation with the degree of cure of the RL as a function of radiation exposure. As shown in Fig. 3, the Tg for the UV standard system increases from 62°C to 82°C. The UV elevated cure system with the secondary cure step at 45°C prior to radiation exposure increases further from 72°C to 90°C, indicating that the initial thermal profile exposure affects the final cure state after radiation. As described by Alessi et al.,¹⁸ a higher thermal treatment after irradiation allows the photoinitiated system to cure more homogeneously than if just cured using radiation as verified by differential scanning calorimetry. This is most likely the reason the subsequent irradiation of the elevated temperature system results in a higher degree of cure than the RT cure system.

This increase in Tg observed for the UV RL caused by radiation exposure may indicate one of the reasons for the improved stability observed in Fig. 2. As described in Table 1, as polymerization increases due to radiation exposure, a number of corresponding mechanical and thermal inherent properties also change. CTE was shown to decrease from 59.6 to 56.5 ppm/m°C while the stiffness was shown to increase from 3.0 to 3.5 GPa. These changes, though limited, would be expected to contribute in favor of increased stability after thermal cycling.

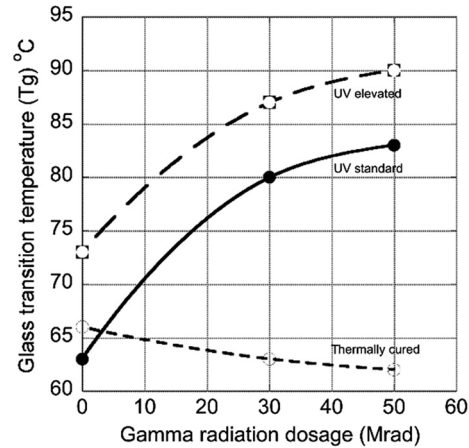


Fig. 3 Tg of various cured resins as a function of radiation dosage.

Table 1 Summary of thermal degradation temperatures for both standard and elevated cured UV resin as a function of radiation exposure.

Cure state	Elastic modulus (GPa)	CTE ppm/m°C	Thermal degradation temperature (°C)	Temperature at 10% weight loss (°C)
UV standard	3.05	59.6	424.7	391.7
UV standard, 50 Mrad	3.43	56.5	427.4	401.6

In comparison, a typical bisphenol-A, thermally processed difunctional, amine-cured system investigated in this study with no photoinitiator showed a decrease in Tg from 66°C to 63°C, over the same exposure levels previously

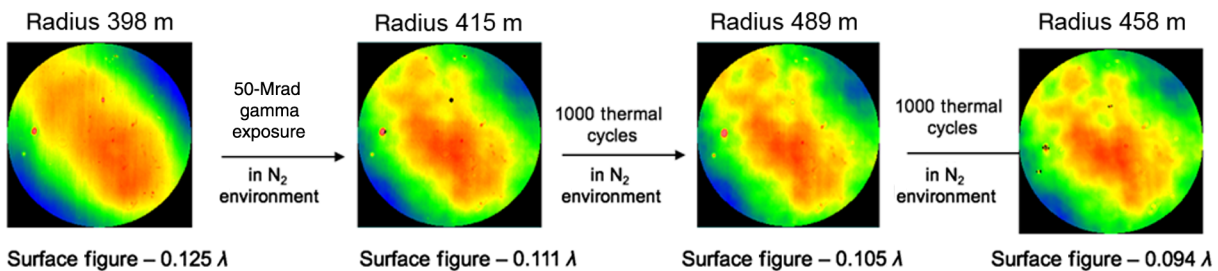


Fig. 2 Zygo analysis of 50-Mrad irradiated, standard cure (RT), UV replicated composite mirror as a function of thermal cycling. Minimal changes observed after both sets of thermal cycles.

described. This suggests fragmentation of the network with radiation for the amine-cured RL. Laricheva¹⁹ made similar observations when exposing an amine-cured epoxy without an initiator to irradiation. His findings showed that the radiation resistance was primarily a function of the radiation resistance of the hardener used. The behavior was quantified by the degree of gas evolution products generated during radiation exposure. The radiation resistance was greatest for hardeners of the following classes: phthalic anhydride, maleic anhydride, methaphenylene diamine, and hexamethylene diamine. Epoxy oligomers with unsaturated compounds also contributed to radiation resistance of the overall structure but to a lesser degree.

Thermal gravimetric analysis (TGA) provides material information with regards to weight loss as a function of temperature. A material that is more cross-linked will exhibit a higher thermal degradation temperature, while one with increased fragmentation will result in an earlier onset of weight loss. The total mass loss may also be affected when more significant structural changes occur. Figure 4 shows a TGA profile for the UV standard control with no radiation exposure. As shown, the thermal degradation temperature is 424.6°C while the temperature at 10% weight loss is ~391.6°C. Table 1 also summarizes the effect of irradiation on the thermal degradation behavior of the UV-cured specimen. As shown, the thermal degradation temperature increases with radiation exposure. This corroborates the Tg data and also verifies that the RL is continuing to cross-link with radiation and does not appear to be fragmenting as was the case for the amine-cured system.

GC-MS was then performed to provide more detailed structural information regarding the effect of radiation on the chemical structure of the starting material. GC-MS allows molecular weight determination of specific components within a formulation. The effect of radiation exposure on the UV RL material was analyzed using GC-MS, pre- and postirradiation. Figure 5 shows scans for the UV-uncured monomer and the UV standard cured material. The various peaks identify the molecular weights of the components

observed in the formulation. As shown in Fig. 5(c), peaks corresponding to the starting materials are indicated by #1 and #2. The peak #1 denotes 4-methyl-4-(glycidyloxyphenyl)-2-pentanone and peak #2 denotes a large bisphenol-like epoxide structure. The peak shown at 13.5 min is related to the photoinitiation sulfonium salt complex as well as the polymerization product. The peak at 22.2 min is also a reaction product due to polymerization.

Figures 6(a) and 6(b) show that even after UV exposure there remains evidence of both of the starting material components at fairly high concentrations, which is consistent with the measured Tg's. This is even the case after a 45°C elevated temperature cure profile. However, after 50 Mrad of exposure, Fig. 6 shows a fairly complete consumption of the starting materials due to added polymerization. This corroborates the increases in modulus, Tg, and thermal degradation measurements previously described for the UV irradiated specimens.

Even though the cure state increases with radiation exposure, other factors may also be contributing to the stability observed after radiation exposure. An increase in cure state alone would not necessarily provide the stability necessary if the residual stresses generated during processing were too large in magnitude. The processing temperatures required to achieve a sufficiently high degree of cure may result in a loss of flatness due to a build-up of residual stresses as was shown for the thermally cured system. A process maintaining a balance between achieving a sufficiently high degree of cure state while minimizing the stress state of the RL is vital to ensure the part remains stable over the intended lifetime period and environmental/thermal exposures.

To evaluate what effect radiation exposure has on the residual stress state of the stack up, a number of UV-coated silicon bimaterial specimens were manufactured and subjected to radiation exposure. Figure 7 shows the replicated resin film stress for the various RL systems investigated as a function of radiation dose. In this figure, we show the calculated film stress for a UV standard cure (RT),

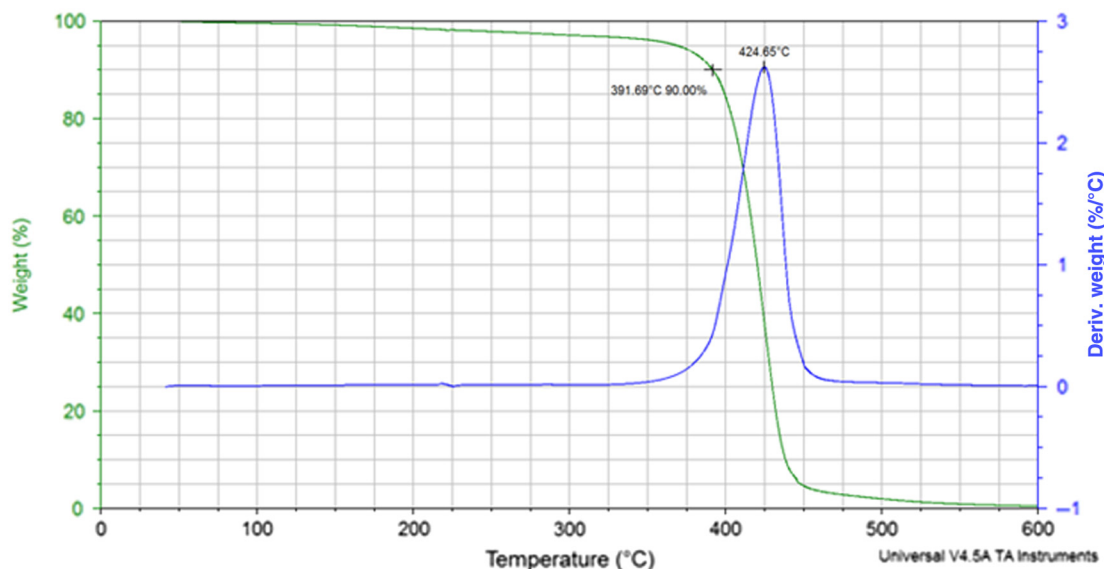


Fig. 4 TGA Profile of UV standard cure RL with no radiation exposure.

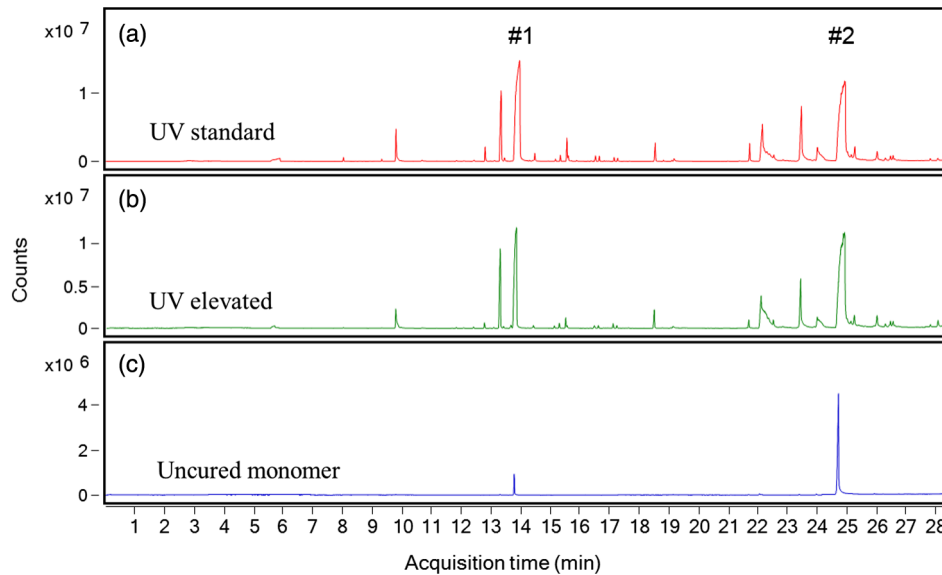


Fig. 5 GC-MS of the UV starting monomer and cured resin materials investigated in this study. Spectra for the (a) UV cured at RT, (b) UV cured + postcure, and (c) uncured monomer are shown. Peaks indicated by #1 and #2 are the starting material.

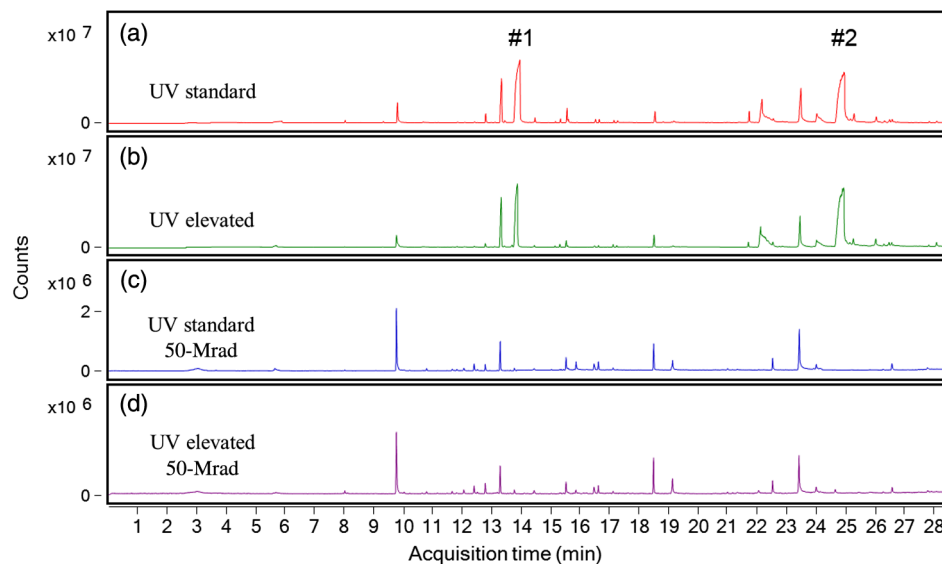


Fig. 6 GC-MS of standard and elevated UV-cured materials: (a, b) pre- and (c, d) post-50-Mrad irradiation.

a UV elevated cure (45°C), and a thermally cured amine epoxy system (45°C). The UV elevated cure was included to show the effect of increasing the processing temperature on the residual stress state of the same material. The RL film stress on a silicon wafer was calculated using the Stoney equation as described in Sec. 2

As shown, the initial film stress is largest for the amine-cured system at 9.5 MPa. This is a result of both the processing temperature (45°C) necessary for sufficient cure to be achieved as well as cure shrinkage. The UV-cured film processed at RT is virtually stress-free. Increasing the cure temperature to an elevated temperature (45°C) for the UV system increases the stress state of the film to 5.5 MPa, which, though higher than the RT cured, remains ~50% lower than that of the thermally cured amine epoxy.

As the dosage of radiation exposure increases to 30 Mrad, all of the RL investigated show a gradual decrease in residual stress that asymptote to a lower stress state based on their initial value. Radiation exposure decreases the overall residual tensile stress state of all the systems investigated. We believe that all of the resins investigated in this study experience some degree of chain scission as a function of gamma radiation exposure. This fragmentation possibly contributes to a reduction of the original film stress with gamma exposure. However, as previously described, the gamma radiation also yields a “net positive increase” in the degree of cure for the UV systems due to the activation of the photoinitiator, which promotes further cross-linking. On the other hand, the amine-cured system does not show a net increase since radiation does not appear to induce further

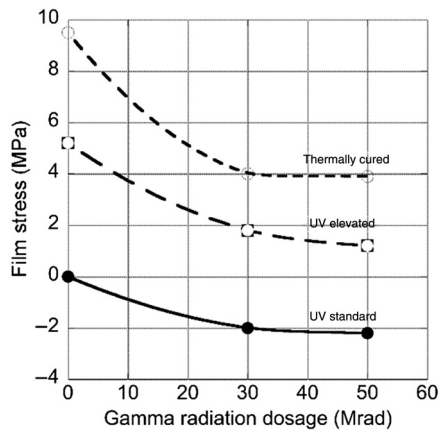


Fig. 7 The effect of radiation on the residual stress of various RLs on silicon wafers using the Stoney equation.

cross-linking. Additional radiation exposure above 30 Mrad showed very little additional changes in the residual stress state of the RL.

To observe the impact of the gamma radiation on critical mirror parameters, including SFE and roughness, mirrors were manufactured on composite substrates using the UV- and the amine-cured epoxies. These samples were then exposed to varying levels of radiation and analyzed by Zygo surface interferometry. Figure 8 shows a series of Zygo analysis scans for a UV replicated composite mirror that has been exposed to varying dosages of gamma radiation. When we take a closer look at the effect of radiation on the SFE of the elevated cure UV replicated mirror, we see that the initial SFE of 0.10λ generally improves when evaluating the flatness as shown in Figs. 2(a)–2(e). This improvement or change may be due to the associated decrease in film

stress described previously in Fig. 7. A reduction in film stress could result in the relaxation of the initial profile to a flatter surface. This in conjunction with the higher degree of cure caused by irradiation may explain the improved performance observed as a function of irradiation exposure. In addition, the surface roughness for the UV-cured mirror as a function of irradiation also shows negligible (1.0 to 1.1 nm) changes since no evidence of extensive chain scission was observed.

In comparison, the Zygo analysis scans for an amine-cured epoxy replicated composite mirror exposed to varying dosages of gamma radiation are shown in Fig. 9. As shown, the starting SFE for the control specimen is $\sim 0.073\lambda$. As the radiation exposure increases, the shape of the mirror progressively becomes less flat or more cup-shaped. After 50 Mrad of exposure, the SFE has experienced a nonrecoverable, deviation from its initial flatness by as much as 0.025λ (35%). Even though there is a relaxation of stress with irradiation, the final stress state still far exceeds that for the UV-cured systems investigated in this study. The material degradation observed due to irradiation, which resulted in decreases to Tg and modulus, is consistent with the changes to the flatness. In addition, the amine-cured epoxy material exhibited increases in surface roughness from 1.4 to 3.3 nm further corroborating fine-scale fragmentation of the network. Figure 10 summarizes the percentage changes observed with respect to SFE as a function of radiation dosage for both a UV- and an amine-cured epoxy system.

The stability of a replicated composite mirror is affected by a number of key parameters. Processing mirrors at relatively low temperature allow the material to maintain lower residual stresses than processing at elevated temperatures. Minimizing the initial stress state is a primary consideration when manufacturing this type of hardware; however,

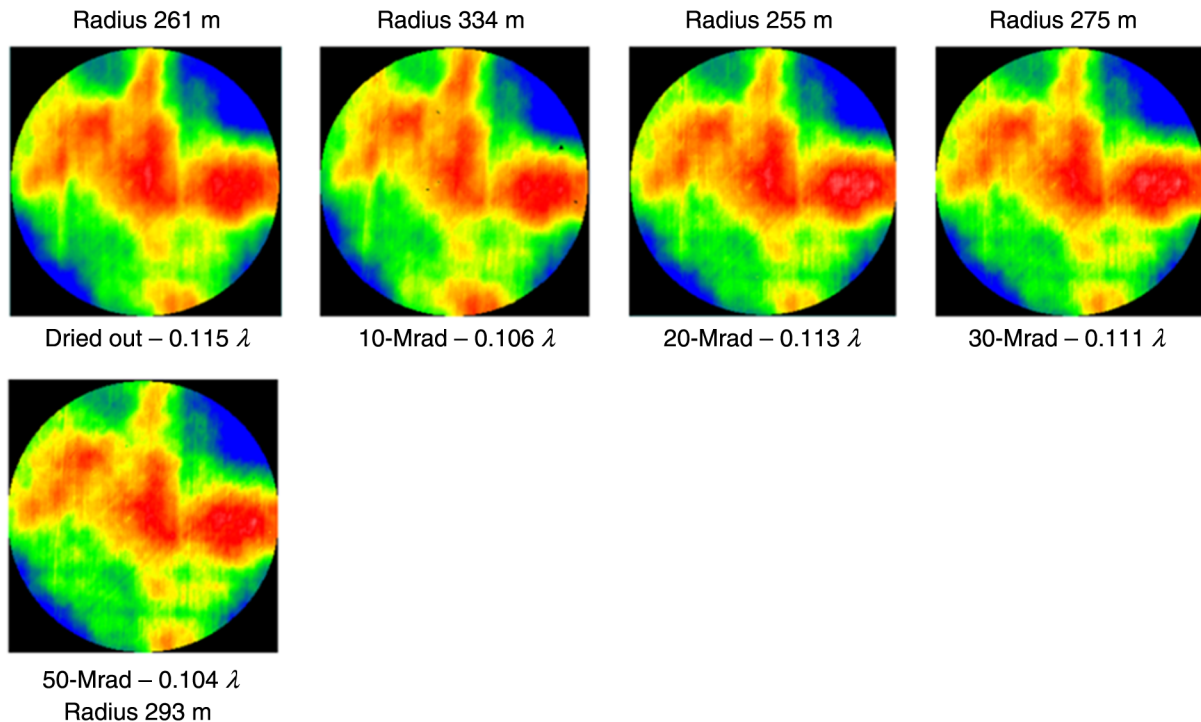


Fig. 8 Zygo analysis of replicated composite mirror as a function of radiation exposure utilizing a UV elevated cured RL system. No significant changes in SFE were observed.

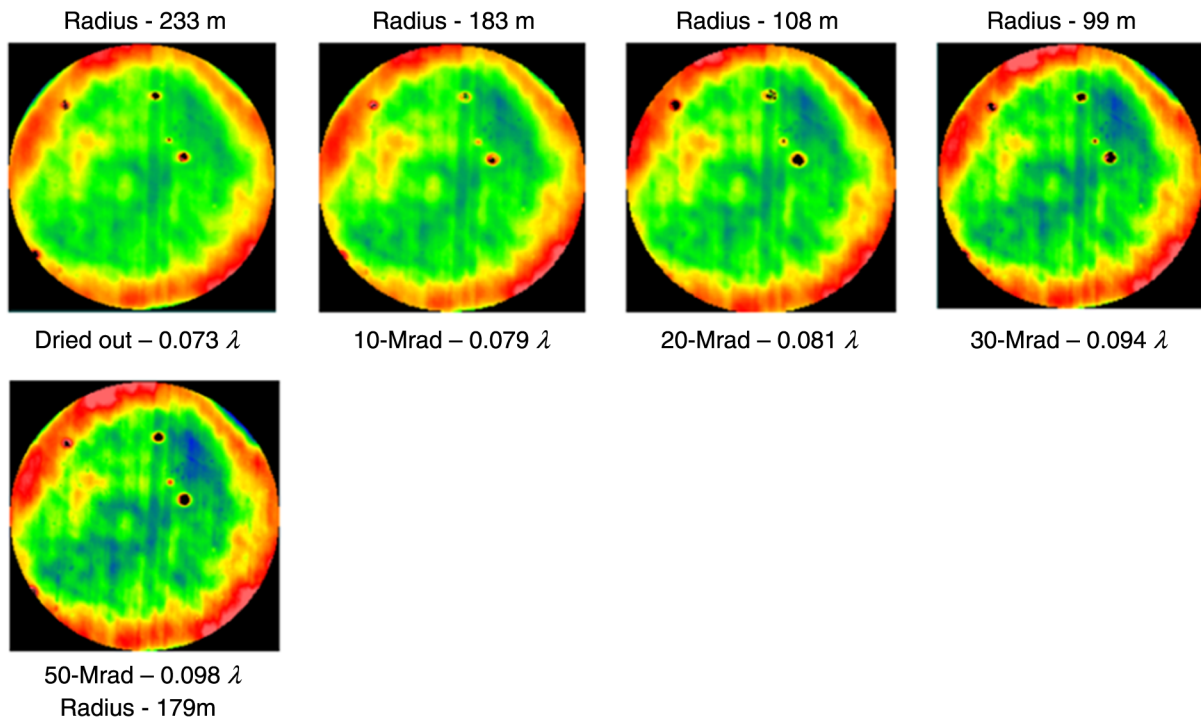


Fig. 9 Zygo analysis of replicated composite mirror as a function of radiation exposure utilizing a thermally cured RL system. Significant increases in SFE were observed with gamma irradiation.

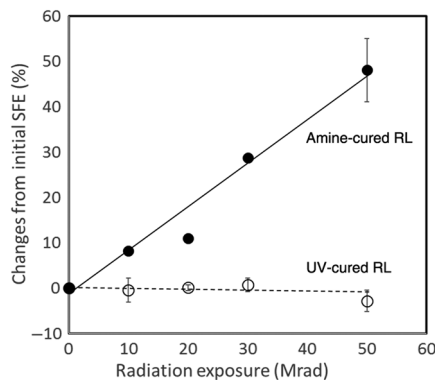


Fig. 10 A plot showing the changes in SFE as a function of radiation exposure. Amine-cured replicated epoxy specimen shows significant increase in SFE, in contrast to UV-cured material showing small improvement in SFE.

a sufficiently high degree of cure must be achieved to attain stability. UV-cured system allows RT cure while attaining a fairly high degree of cure in comparison to comparable thermally cured systems. However, even for the case of UV-cured systems, distortion may occur on a nanometer scale when the degree of cure is limited by low temperature processing (RT). Exposure to gamma radiation was shown to significantly increase the cure state of the UV-cured systems investigated in this study as verified by DMA, TGA, and GC-MS. This increase in cure state with RT processing contributed to material changes (high T_g , high modulus, and low CTE) that provide improvements to mirror stability. Gamma radiation of UV replicated mirrors was also shown to simultaneously reduce the overall film stress as well as further promote cure within the polymer network

by activating the photoinitiator. This is encouraging for space-based applications utilizing these mirrors. Thermally cured epoxy mirrors did show improvement with radiation exposure due to a relaxation of processing stresses; however, both the magnitude of the initial stress state as well as the continued chain scission of the network with irradiation may result in a less stable long-term solution for space-based applications.

4 Conclusion

Composite replicated mirrors are viable replacements for space-based conventional glass mirrors due to their lower density, tailorable mechanical properties, and rapid manufacturing times over state-of-the-art glass mirrors. UV-cured mirrors provide a route by which high-quality mirrors can be manufactured at relatively low processing temperatures minimizing residual stresses when compared to amine-cured epoxies. Gamma radiation treatment of UV systems was shown to promote cure at RT as evidenced by sharp increases in T_g , modulus, and the thermal degradation temperature. Improvements to the cure state due to gamma exposure contribute to the overall stability of the mirror as well as to minimize processing residual stresses. GC-MS of UV-cured material showed that the photoinitiator was activated and consumption of the primary monomers was observed with gamma exposure promoting further cure at RT. In contrast, indications of network fragmentation were observed for the amine-cured epoxy RL system. The same levels of gamma exposure on the amine-cured amine epoxy replicated mirrors resulted in decreased mechanical and thermal performance. The radiation dosage was also shown to reduce the film stress of all of the replicated mirrors manufactured in this study by as much as 80% as evidenced using Stoney replicated specimens. Gamma exposure as a process step

for the manufacture of high stability mirrors was shown to provide significant improvement in mirror stability even after multiple thermal cycling in comparison nonirradiated composite mirrors.

Acknowledgments

This study was funded by Aerospace Corporation's sustained experimentation and research for program applications.

References

1. S. Teare et al., "An adaptively corrected composite material telescope," *SPIE Newsroom* (2006).
2. P. Chen et al., "Advances in very lightweight composite mirror technology," *Opt. Eng.* **39**(9), 2320–2329 (2000).
3. C. Miao et al., "Shear stress in magnetorheological finishing for glasses," *Appl. Opt.* **48**, 2585–2594 (2009).
4. H. Kim et al., "Evaluating the use of self-assembled monolayer (SAM) release coating for replicated optics," *J. Adhes. Sci. Technol.* **30**(23), 2544–2556 (2016).
5. G. L. Ferrelli, H. I. Kim, and R. J. Zaldivar, "Lightweight replicated composite mirrors using UV cured resin," in *Composites and Advanced Materials Expo (CAMX) Conf. Proc.*, Anaheim, California (2016).
6. R. J. Zaldivar, G. L. Ferrelli, and H. I. Kim, "Hygroscopic and thermal stability of high precision replicated epoxy composite mirrors," *Opt. Eng.* **56**(11), 117103 (2017).
7. G. L. Ferrelli, "Effect of resin cure on the stability of high-quality replicated composite mirror surface," MS Thesis, University of California Los Angeles, Los Angeles, California (2017).
8. J. V. Crivello, "UV and electron beam-induced cationic polymerization," *Nucl. Instrum. Methods Phys. Res. Sect. B* **151**, 8–21 (1999).
9. J. V. Crivello, "Advanced curing technologies using photo- and electron beam induced cationic polymerization," *Radiat. Phys. Chem.* **63**, 21–27 (2002).
10. H. W. Bonin et al., "Effects of high radiation environments on polymer composite epoxies," in *Int. Nuclear Congress (INC) Proc.*, Canada, Vol. 3, p. 1500 (1993).
11. S. Alessi et al., "Ionizing radiation induced curing of epoxy resin for advanced composites matrices," *Nucl. Instrum. Methods Phys. Res. Sect. B* **236**, 55–60 (2005).
12. J. O'Donnell et al., "Chain scission and cross-linking in the radiation degradation of polymers: limitations on the utilization of theoretical expressions and experimental results in the Pregel region," *Macromolecules* **12**(1), 113–119 (1979).
13. W. J. Chappas et al., "EB curing of maritime composite structures," *Radiat. Phys. Chem.* **56**, 417–427 (1999).
14. D. Abliz et al., "Curing methods for advanced polymer composites—a review," *Polym. Polym. Compos.* **21**(6), 341–348 (2013).
15. G. Spadaro et al., "Novel epoxy formulations for high energy radiation curable composites," *Radiat. Phys. Chem.* **72**, 465–473 (2005).
16. T. Q. Cao et al., "Feasibility study of electron beam cured composites," in *Proc. of the 46th Int. SAMPE Technical Symp.*, Seattle, Washington, DC, pp. 862–873 (1996).
17. C. Dispenza et al., "High energy radiation cure of resin systems for structural adhesives and composite applications," *Radiat. Phys. Chem.* **63**, 69–73 (2002).
18. S. Alessi et al., "The influence of the processing temperature on gamma curing of epoxy resins for the production of advanced composites," *Radiat. Phys. Chem.* **76**, 1347–1350 (2007).
19. V. P. Laricheva, "Effect of ionizing radiation on epoxy oligomers of different structures and manufacture of new promising materials on their base," *Radiat. Phys. Chem.* **77**, 29–33 (2008).

Rafael J. Zaldivar is the director of the Materials Science Department at The Aerospace Corporation. He received his PhD in materials science and engineering from the University of California, Los Angeles (UCLA) in 1992. His research interests include composite optics, composite materials processing, plasma surface treatment of carbon materials, and 3-D additive manufacturing. He holds 12 patents in these various technology areas.

Hyun I. Kim is a research scientist at The Aerospace Corporation. He obtained a BS degree in chemistry from the University of Texas at Austin in 1994 and his PhD in chemistry from the University of Houston in 1999. After two years of postdoctoral fellowship at Sandia National Laboratories, he joined The Aerospace Corporation in 2001. His research interest includes surface engineering of composite materials.

Geena L. Ferrelli is a member of technical staff at The Aerospace Corporation in the Materials Science Department, working specifically with polymers and composites. She received her MS degree in materials science from UCLA, and she is currently pursuing her PhD at UCLA, focusing on replicated composite optics.